DOI 10.1007/s11595-016-1482-9

Effect of Corrosive Solutions on C-S-H Microstructure in Portland Cement Paste with Fly Ash

DING Qingjun[1], WANG Huan[1], HU Chenguang[2], ZHANG Gaozhan[1,3]*

(1. School of Materials Science and Engineering, Wuhan University of Technology, Wuhan 430070, China; 2. College of Materials Science and Engineering, North China University of Science and Technology, Tangshan 063000, China; 3. School of Materials and Chemical Engineering, Anhui Jianzhu University, Hefei 230601, China)

Abstract: By means of ^{29}Si and ^{27}Al magic angle spinning nuclear magnetic resonance (MAS NMR) combined with deconvolution technique, X-ray diffraction (XRD), scanning electron microscopy (SEM) as well as energy dispersive X-ray system(EDX), the effect of 5 wt% corrosive solutions (*viz*. 5 wt% Na_2SO_4, $MgSO_4$, Na_2SO_4+NaCl and Na_2SO_4+NaCl+Na_2CO_3) on C-S-H microstructure in portland cement containing 30 wt% fly ash was investigated.The results show that, in $MgSO_4$ solution, Mg^{2+} promotes the decalcification of C-S-H by SO_4^{2-},increasing silicate tetrahedra polymerization and mean chain length (MCL) of C-S-H. However, the substituting degree of Al^{3+} for Si^{4+} (Al[4]/Si) in the paste does not change evidently. Effect of Na_2SO_4 solution on C-S-H is not significantly influenced by NaCl solution, while the MCL and Al[4]/Si of C-S-H in fly ash-cement paste slightly change. However, the decalcification of C-S-H by SO_4^{2-} and CO_3^{2-} attack, as well as the activation of fly ash by SO_4^{2-} attack will increase the MCL and Al[4]/Si, which are both higher than that under Na_2SO_4 corrosion, $MgSO_4$ or Na_2SO_4 +NaCl coordination corrosion.

Key words: corrosive solutions; cement; fly ash; C-S-H microstructure; Al[4]/Si

1 Introduction

In both sea and western regions of China, there are multiple corrosive ions, such as SO_4^{2-},Mg^{2+}, Cl^- and CO_3^{2-},and coupling interaction of these corrosive ions results in crack and serious durability degradation of concrete, shortening service life and causing enormous economic and resource losses. In concrete, calcium silicate hydrate (C-S-H) as the main hydration product of cement-based materials, is the main strength source of hardened cement pastes[1], however, C-S-H microstructure is short-range order amorphous structure, which will correspondingly change with corrosive ions which directly affects the macroscopic properties of concrete.

However, current researches about the effect of corrosive ions on the concrete microstructure mainly centralize around the species, composition and morphology of corrosive product under ions on the macroscopic mechanical properties, ions diffusion, expansive destruction and so on[2,3], quantitative studies on C-S-H microstructure under multiple ions corrosion are few. Multiple ions corrosion not only improves cement hydration and stimulates the activation of fly ash reactivity, but also influences the distribution of 4-coordinated aluminum (Al[4]) and 6-coordinated aluminum (Al[6]) in cementitious pastes, eventually leading to more complex and changeable C-S-H microstructure.Therefore, the evolution of C-S-H microstructure under multiple corrosive ions is revealed as an important basis to improve the durability and service life of marine concrete. Thus, in this paper, the effect of multiple corrosive ions on C-S-H microstructure in fly ash-cement paste is quantitatively analyzed in order to provide a theoretical basis for the optimization and regulation of the C-S-H microstructure and improve the durability of concrete.

(Received: Oct. 20, 2015; Accepted: July 4, 2016)

DING Qingjun(丁庆军): Prof.; Ph D; E-mail: dingqj@whut.edu.cn

*Corresponding author: ZHANG Gaozhan(张高展): Ph D; E-mail: gaozhanzhang@126.com

Funded by the Major State Basic Research Development Program of China ("973"Program) (No. 2015CB655101), Natural Science Foundation of Hebei (No.E2016209283), National Natural Science Foundation of China(No.51402003), and Open Foundation of Road Bridge and Structural Engineering Key Laboratory WHUT, China (No.DQZDJJ201504)

Table 1 Chemical composition of materials /wt%

Materials	CaO	SiO_2	Al_2O_3	Fe_2O_3	SO_3	MgO	TiO_2	Na_2O	K_2O	Other
Cement	62.60	21.35	4.67	3.31	2.25	3.08	0.27	0.21	0.54	0.72
Fly ash	1.60	58.50	32.40	3.01	0.33	0.53	1.18	0.42	1.72	0.04

2 Experimental

2.1 Materials

P.I 52.5 Portland cement from Huaxin (Huangshi, Hubei), and class I fly ash (FA) from Huayuan (Zhenjiang Jianbi Power Plant) were used, the chemical compositions are listed in Table 1. Mixing water was distilled water. Na_2SO_4, $MgSO_4$, NaCl and Na_2CO_3 were chemical pure reagents. According to the ASTM C-1012[6], 5 wt% Na_2SO_4, $MgSO_4$, NaCl and Na_2CO_3 solution were prepared as corrosive solutions.

2.2 Preparation

Cement paste containing 30 wt% fly ash (water-cement ratio at 0.35) was prepared and molded in the Φ10 mm ×50 mm plastic pipe (one side sealed by rubber plug). The samples were demoulded after standard curing for 24 h, and the sample surface was covered evenly with epoxy resin except for the one contacted with the rubber plug. These samples were immersed in plastic-sealed box containing corrosive solutions (5 wt% Na_2SO_4, $MgSO_4$, Na_2SO_4+NaCl and Na_2SO_4+NaCl+Na_2CO_3), and then cured in the standard curing room.Then samples were removed after 540 d. Outside layer with about 2 mm thickness was cut off, cracked to particle size less than 3 mm, and immersed in absolute alcohol for 1 d. Finally,they were ground to fine powder and stored in a vacuum dryer at 50 ℃ for 2 h .

2.3 Test methods

2.3.1 ^{29}Si and ^{27}Al NMR

Bruker Advanced III 400WB spectrometer (magnetic field 9.4 T; operating frequency of 79.5 MHz for ^{29}Si and of 10^4 MHz for ^{27}Al) was employed to quantitatively analysize C-S-H microstructure. Samples were packed into 4 mm broadband probes and span at 8 kHz for ^{29}Si and 12 kHz for ^{27}Al. The ^{29}Si pulse width was 2 μs, the pulse delay was 2 s, and acquisition length was 42.6 ms.The ^{27}Al pulse width was 1 μs, the pulse delay was 1s, and acquisition length was 25.0 ms.The ^{29}Si and ^{27}Al chemical shifts were respectively referred against external samples of the tetramethylsilane (TMS) and $Al(NO_3)_3$, 1 M, at 0 ppm.

2.3.2 XRD

X-ray diffraction (XRD): D/MAX2500PC, produced by Japanese Rigaku Corporation,was used to analyse the phases present in the pastes, including any deterioration products. The hardened fly ash-cement pastes were ground to particle size less than 75 μm. The analyses were performed between 5 and 65° at a speed of 2° /min with Cu(Kα) ray in 100 mA and 40 kV.

2.3.3 SEM-EDX

The microstructure of fractured surface samples was examined using the field emission scanning electron microscope (FESEM), produced by Japan Hitachi Company, with 20 kV acceleration voltage. The chemical analysis was carried out using an energy dispersive X-ray (EDX) system and the appropriate Link software, produced by America Thermo Company.

3 Results and discussion

3.1 ^{29}Si NMR analysis of cement and fly ash

Quantitative information on the fractions of Si site in silicate tetrahedra with different connectivity was obtained by ^{29}Si MAS NMR spectra. Q^n (n = 0-4) denotes the connectivity of the silicate tetrahedron[8,9]. Q^0 represents isolated tetrahedra, which presents in the anhydrous silicate minerals in cement. Q^1 represents chain-end dimeric tetrahedra group or polymeric silicate units. Q^2 represents the middle-chain groups, including the 'paired' tetrahedra (Q^{2P}) and 'bridging' tetrahedra (Q^{2B})[4]. Q^2(1Al) represents middle-chain groups where one of the adjacent tetrahedra is occupied by aluminum[4-6]. Q^3 represents tetrahedron connected with the other three [SiO_4], which is a double chain polymeric structure or layered structure with a chain branching; Q^4 represents three dimensional network structure with four [SiO_4] [7].

The deconvolution technology was applied to assign resonances to individual species by Peakfit v4.12 software. In addition, the hydration degree of silicate minerals in portland cement (α_C), reaction degree of fly ash(α_{FA}), the mean chain length (MCL) of C-S-H, and the substituting degree of Al^{3+} for Si^{4+} (Al[4]/Si ratio) were calculated by the following Eqs.(1), (2), (3) and (4), respectively[8]:

$$\alpha_c=1-I(Q_0)/I_0(Q^0) \quad (1)$$

$$\alpha_{FA}=1-I(Q^3+Q^4)/I_0(Q^3+Q^4) \quad (2)$$

$$MCL=2[I(Q^1)+I(Q^2)+1.5I(Q^2(1Al))]/I(Q^1) \quad (3)$$

$$Al[4]/Si=0.5I(Q^2(1Al))/[I(Q^1)+I(Q^2(0Al))+I(Q^2(1Al))] \quad (4)$$

where $I_0(Q^0)$ and $I(Q^0)$ are the integral intensity of Q^0 in cement and the hydrated cement pastes. $I_0(Q^3+Q^4)$ and $I(Q^3+Q^4)$ are integral intensity of Q^3+Q^4 in fly ash and fly ash-cement pastes. $I(Q^1)$, $I(Q^2)$ and $I(Q^2(1Al))$ are the integral intensity of Q^1, Q^2 and $Q^2(1Al)$ in C-S-H, respectively.

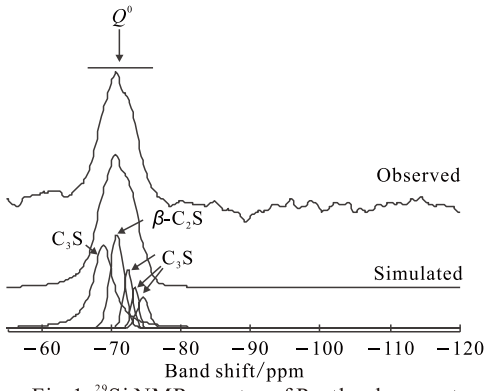

Fig.1 ^{29}Si NMR spectra of Portland cement

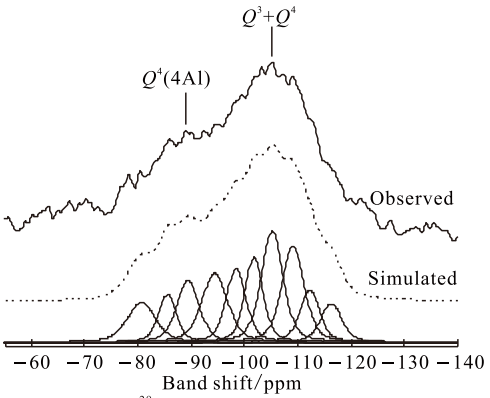

Fig.2 ^{29}Si NMR spectra of fly ash

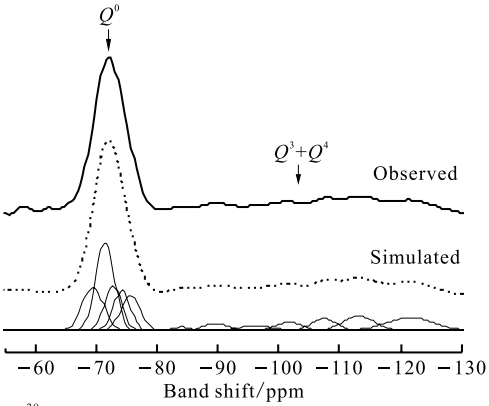

Fig.3 ^{29}Si NMR spectra of 30%fly ash-cement materials

^{29}Si NMR spectra of cement,fly ash and cement containing 30%fly ash are respectively presented in Fig.1, Fig.2 and Fig.3. As shown in Fig.1, the resonance lines around −68.8, −72.3, −73.3, −74.5 ppm are attributed to Q^0 site in C_3S phase,and the peak around −70.7 ppm is attributed to Q^0 site in C_2S phase[8]. From Fig.2, the resonance lines around −84, −93.8, −98.6, −103.4 and −108 ppm are assigned to vitreous in fly ash[9], and the resonance lines around −88 and −114 ppm are attributed, respectively, to Q^4(4Al) in mullite[9] and Q^4(0Al) in quartz[9]. By deconvolution calculation from Fig.3, the integral intensities of Q^0 in cement and Q^3+Q^4 in fly ash reach 67.60% and 32.40%, respectively.

3.2 Effect of corrosive solutions on hydration degree of silicate minerals and reaction degree of fly ash

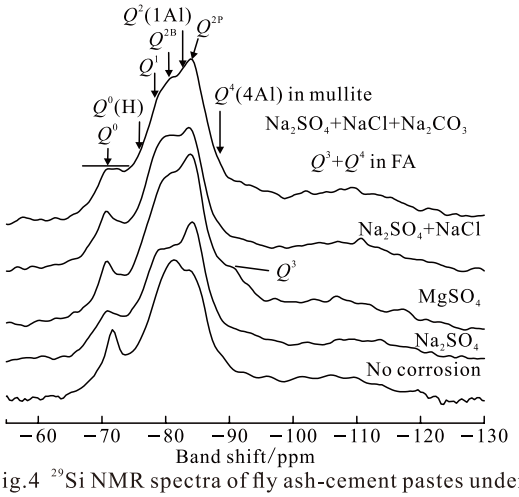

Fig.4 ^{29}Si NMR spectra of fly ash-cement pastes under corrosive solutions for 540 d

^{29}Si NMR spectra of fly ash-cement pastes under corrosive solutions for 540 d are shown in Fig.4, and the integral intensity of Q^n and deconvolution calculation results are presented in Table 2 and Table 3.

As can be seen from Table 3, the hydration degree of silicate minerals under $MgSO_4$ solution corrosion is close to Na_2SO_4 solution corrosion, while the reaction degree of fly ash is opposite, which indicates that Mg^{2+} involved in $MgSO_4$ solution corrosion has little promotion effect on silicate mineral hydration and activation of fly ash ,because of the formation of $Mg(OH)_2$ (MH) thin layer and silica gel[10] (shown as Eqs.5, 6, and 7 and confirmed from Fig.4: ^{29}Si NMR of $MgSO_4$ solution corrosion has Q^3 site in chemical shift about −93 ppm) on the paste surface, filling paste pore to hinder penetration and diffusion of SO_4^{2-}, and reducing the formation of gypsum and AFt. It can also be proved from Fig.5 that the diffraction intensity of gypsum and AFt in paste under $MgSO_4$ solution corrosion is significantly lower than Na_2SO_4 solution

Table 2 Relative intensity of Q^n from ^{29}Si NMR spectra in Fig. 4

Samples	The relative intensity of Q^n/%						
	Q^0	Q^0(H)	Q^1	Q^2(1Al)	Q^2B	Q^2P	Q^3+Q^4
No corrosion	12.79	1.06	33.38	10.12	6.05	12.07	24.53
Na_2SO_4	11.94	0.98	19.60	14.19	9.83	19.66	23.80
$MgSO_4$	11.32	1.88	18.14	13.22	10.39	20.67	24.38
Na_2SO_4+NaCl	11.55	1.96	19.61	15.76	9.25	18.45	23.42
Na_2SO_4+NaCl+Na_2CO_3	10.84	1.72	12.46	18.85	11.25	22.15	22.72

Table 3 Calculation results from deconvolution of ^{29}Si NMR spectra in Table 2

Samples	α_C/%	α_{FA}/%	MCL	Al[4]/Si
No corrosion	81.08	24.28	4.00	0.082
Na_2SO_4	82.34	26.55	7.18	0.112
$MgSO_4$	83.13	24.74	10.51	0.113
Na_2SO_4+NaCl	82.91	27.71	7.24	0.115
Na_2SO_4+NaCl+Na_2CO_3	83.96	29.88	11.90	0.146

corrosion, but the diffraction intensity of AFm is higher. However, the diffraction peak of $Mg(OH)_2$ is not obviously observed in XRD patterns after $MgSO_4$ solution corrosion, which illustrates the formation of M-S-H gel (Eq.8) rather than MH .

$$M\bar{S}+CH+2H\rightarrow C\bar{S}H_2+MH \quad (5)$$

$$C-S-H+M\bar{S}+5H\rightarrow MH+C\bar{S}H_2+S_2H \quad (6)$$

$$C_4AH_{13}+3M\bar{S}+2CH+20H\rightarrow C_3A\cdot 3C\bar{S}\cdot H_{32}+3MH \quad (7)$$

$$2MH+S_2H\rightarrow M\text{-}S\text{-}H \quad (8)$$

For the paste under Na_2SO_4+NaCl solution corrosion, due to that the diffusion rate of Cl^- is two orders of magnitude higher than SO_4^{2-}[11], Cl^- firstly enters into the paste and reacts with the calcium aluminum hydrate (CAH) or AFm to form(proved from Fig.5: the intensities of gypsum and AFt diffraction peaks are significantly lower, and diffraction peaks are found), and the amount of Cl^- involved in Na_2SO_4+NaCl solution corrosion is reduced. Therefore the hydration degree of silicate mineral and activation of fly ash under Na_2SO_4+NaCl solution corrosion are close to that of Na_2SO_4 solution corrosion.

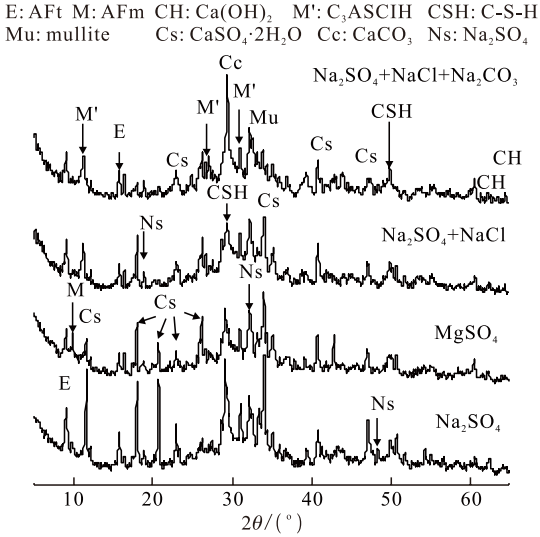

Fig.5 XRD patterns of 30%fly ash-cement pastes under corrosive solutions for 540 d

As shown in Table 3, CO_3^{2-} involved in Na_2SO_4+NaCl+Na_2CO_3 solution corrosion accelerates the activation effect of SO_4^{2-} on silicate minerals and fly ash. It is because that CO_3^{2-} combines a large number of CH to form $CaCO_3$. Alkalinity in paste is reduced and hydration degree of the silicate minerals is also improved. At the same time, the consumption of CH by CO_3^{2-} decreases formation amount of gypsum (Fig.5), and promotes the activation effect of SO_4^{2-} on fly ash.

3.3 Effect of corrosive solutions on mean chain length of C-S-H in fly ash-cement pastes

As shown in Table 3, the MCL (10.51) of C-S-H under $MgSO_4$ solution corrosion is higher than that under Na_2SO_4 solution corrosion (7.18). Compared the intensity of Q^n in fly ash-cement pastes under Na_2SO_4 solution corrosion, intensities of Q^0 and Q^1 respectively decrease by 0.62% and 1.46%.It means that in spite of lower promotion effect of $MgSO_4$ solution corrosion on hydration of silicate minerals, the decalcification decreases the amount of dimer, resulting in the increase of MCL. Nevertheless, due to higher diffusion coefficient of Cl^- and formation of stable Friedl's salt, the MCL (7.24) of C-S-H under Na_2SO_4+NaCl solution corrosion is close to that under Na_2SO_4 solution

corrosion (7.18). The MCL (11.90) of C-S-H of the paste under Na_2SO_4+NaCl+Na_2CO_3 solution corrosion is totally higher than that under other solutions because of the evident decalcification of C-S-H caused by CO_3^{2-} and SO_4^{2-}.

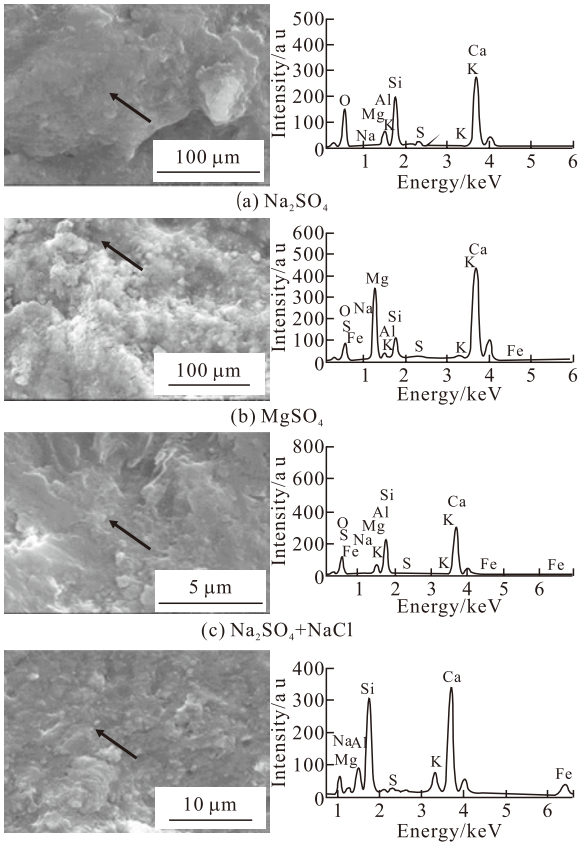

Fig.6 SEM images of 30%fly ash-cement pastes under corrosive solutions for 540 d

Through the SEM-EDX analysis of pastes under corrosive solutions (Fig.6), the C-S-H of paste under $MgSO_4$ solution corrosion shows loose granular packing, and a large amount of magnesiums are observed by EDX, demonstrating the formation of M-S-H gel. Meanwhile, Ca/Si ratio of C-S-H under Na_2SO_4 solution corrosion is similar with Na_2SO_4+NaCl solution corrosion, whereas Ca/Si ratio of C-S-H under Na_2SO_4+NaCl+Na_2CO_3 solution corrosion is rather lower, which is in consistent with the calculation result of MCL.

3.4 Effect of corrosive solutions on substituting degree of Al^{3+} for Si^{4+} in C-S-H

As can be seen from Table 3, Al[4]/Si of C-S-H in pastes under Na_2SO_4, $MgSO_4$ and Na_2SO_4+NaCl solution corrosion all similar, but higher than that under no corrosion. However, due to the activation of fly ash by SO_4^{2-} and dealuminization of CO_3^{2-}, Al[4]/Si of C-S-H under Na_2SO_4+NaCl+Na_2CO_3 solution corrosion is higher than that under Na_2SO_4 solution corrosion.

^{27}Al NMR spectra of fly ash and pastes under corrosive solutions are presented in Fig.7 and Fig.8. The integral intensity and deconvolution calculation results are presented in Table 4. According to Fig.7 and Fig.8, the aluminum in fly ash existed as Al[4], Al[5] and Al[6] in mullite.The peaks of chemical shifts at about 50.0 ppm(■), 36.0 ppm(▲) and 0.9 ppm(★) correspond to Al[4], Al[5] and Al[6] in mullite, and the peaks of chemical shifts at about 67.2 ppm(●) , 13.2 ppm, 9.0 ppm and 3.8 ppm are, respectively, attributed to Al[4] of bridging silicate tetrahedra in C-A-S-H, ettringite, monosulphate and the third aluminate hydrate (TAH). TAH is a cementitious aluminate phase or calcium aluminate hydrate, which mainly consists of $Al(OH)_6^{3-}$ octahedral units .

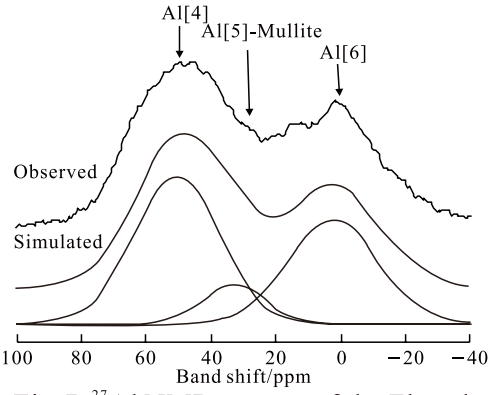

Fig.7 ^{27}Al NMR spectra of the Fly ash

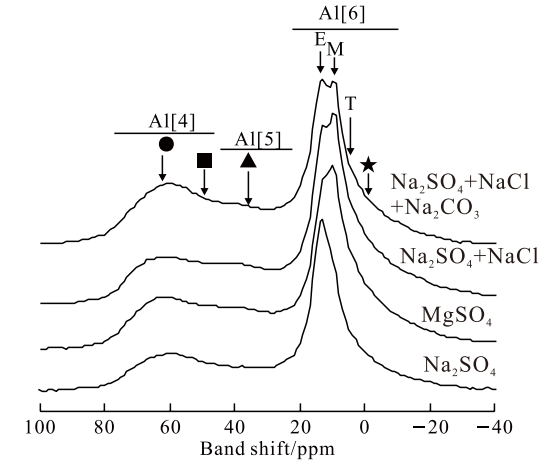

Fig.8 ^{27}Al NMR spectra of 30%fly ash-cement pastes under corrosive solutions for 540 d

As shown in Table 4, due to the formation of silica gel or M-S-H by $MgSO_4$ solution corrosion filling the pore and reducing the dealuminization of SO_4^{2-} on C-A-S-H, the integral intensity of Al[4] (14.27%) in C-S-H under $MgSO_4$ solution corrosion

Table 4 Deconvolution data of ^{27}Al NMR spectra from Fig.8

Samples	The relative intensity of Al^{3+} coordination/%						
	Al[4]-●	Al[4]-■	Al[5]-▲	Al[6]-E	Al[6]- M	Al[6]- T	Al[6]-★
Na_2SO_4	13.20	11.19	10.30	37.64	12.44	4.37	10.87
$MgSO_4$	14.27	11.65	18.11	17.25	19.41	7.31	11.98
Na_2SO_4+NaCl	15.17	8.29	17.58	17.83	15.40	7.79	17.93
Na_2SO_4+NaCl+Na_2CO_3	21.61	8.86	18.69	21.52	11.13	4.79	13.41

is higher than that under Na_2SO_4 solution corrosion (13.20%), but the integral intensity of AFt is opposite. However, the relative intensity of Al[4] in C-S-H under Na_2SO_4+NaCl solution corrosion is close to that under Na_2SO_4 solution corrosion, and the integral intensity of AFm in paste under Na_2SO_4+NaCl solution corrosion is higher.It is because the formation of Friedl's salt promotes the transformation from AFt to AFm, thus weakening the dealuminization of SO_4^{2-} on C-A-S-H. In addition, it is noticeable that the integral intensity of Al[4] (21.61%)under Na_2SO_4+NaCl+Na_2CO_3 solution corrosion is higher than that under Na_2SO_4+NaCl solution corrosion(15.17%), which illustrates that the decalcification of CO_3^{2-} on C-S-H increases polymerization, thus improving the binding effect of C-S-H on Al[4] and dealuminization resistance of C-A-S-H.

4 Conclusions

a) Under $MgSO_4$ solution corrosion, the activation effect of $MgSO_4$ solution corrosion on silicate minerals and fly ash is not significant. Mg^{2+} promotes the decalcification of SO_4^{2-} on C-S-H, enlarging silicate tetrahedra polymerization, thus increasing MCL of C-S-H. However, compared with Na_2SO_4 solution corrosion, Al[4]/Si in C-S-H increases a little under $MgSO_4$ solution corrosion.

b) Cl^- involved in Na_2SO_4+NaCl solution corrosion has little activation effect on silicate minerals and fly ash. Moreover, MCL and Al[4]/Si of C-S-H change slightly.

c) Under Na_2SO_4+NaCl+Na_2CO_3 solution corrosion, the decalcification of CO_3^{2-} accelerates the activation effect of SO_4^{2-} on silicate minerals and fly ash. In addition, the decalcification of both SO_4^{2-} and CO_3^{2-} on C-S-H and activation of SO_4^{2-} and Cl^- on fly ash increase MCL and Al[4]/Si of C-S-H.

References

[1] Taylor H F W. *Cement Chemistry. 2nd*[M]. London: Thomas Telford, 1997

[2] Irassar E F, Bonavetti V L, Gonzalez M. Microstructural Study of Sulfate Attack on Ordinary and Limestone Portland Cements at Ambient Temperature[J]. *Cement and Concrete Research*, 2003, 33(1): 31-41

[3] El-Hachem R, Rozière E, Grondin F, *et al.* New Procedure to Investigate External Sulphate Attack on Cementitious Materials[J]. *Cement and Concrete Composites*, 2012, 34(3): 357-364

[4] Richardson I G, Brough A R, Brydson R, *et al.* Location of Aluminum in Substituted Calcium Silicate Hydrate (C-S-H) Gels as Determined by ^{29}Si and ^{27}Al NMR and EELS[J]. *Journal of the American Ceramic Society*, 1993, 76(9): 2 285-2 288

[5] Richardson I G. The Nature of CSH in Hardened Cements[J]. *Cement and Concrete Research*, 1999, 29(8): 1 131-1 147

[6] Richardson I G. Tobermorite/jennite-and Tobermorite/calcium Hydroxide-based Models for the Structure of CSH: Applicability to Hardened Pastes of Tricalcium Silicate, β-Dicalcium Silicate, Portland Cement, and Blends of Portland Cement with Blast-furnace Slag, Metakaolin, or Silica Fume[J]. *Cement and Concrete Research*, 2004, 34(9): 1 733-1 777

[7] He Y J, Hu S G. Application of ^{29}Si Nuclear Magnetic Resonance (NMR) in Research of Cement Chemistry[J]. *Journal of Materials Science and Engineering*, 2007, 25(1): 147-153 (in Chinese)

[8] Grimmer A R. Structural Investigation of Calcium Silicates from ^{29}Si Chemical Shift Measurements[M]. In: P. Colombet, A-R. Grimmer (Eds.), *Application of NMR Spectroscopy to Cement Science*. London: Gordon and Breach, 1994

[9] Fernández-Jiménez A, Palomo A, Sobrados I, *et al.* The Role Played by the Reactive Alumina Content in the Alkaline Activation of Fly Ashes[J]. *Microporous Mesoporous Materials*, 2006, 91: 111-119

[10] Bonen D, Cohen M D. Magnesium Sulfate Attack on Portland Cement Paste II. Chemical and mineral analysis[J]. *Cement Concrete Research*, 1992, 22(2), 707-718

[11] García-Lodeiro I, Fernández-Jiménez A, Palomo A, *et al*. Effect on Fresh C-S-H Gels of the Simultaneous Addition of Alkali and Aluminum[J]. *Cement Concrete Research*, 2010, 40: 27-32